



RESEARCH ARTICLE | JANUARY 17 2024

Interfacial engineering to manipulate the effective spin Hall angle of perpendicularly magnetized systems

Saikat Maji ; Kartikey Pratap Chauhan ; Ishan Bhat ; Ankan Mukhopadhyay ; Soubhik Kayal ; P. S. Anil Kumar  



Appl. Phys. Lett. 124, 032402 (2024)

<https://doi.org/10.1063/5.0181184>



View
Online



Export
Citation

CrossMark



Applied Physics Letters

Special Topic:
Advances in Quantum Metrology

Submit Today

Interfacial engineering to manipulate the effective spin Hall angle of perpendicularly magnetized systems

Cite as: Appl. Phys. Lett. **124**, 032402 (2024); doi: [10.1063/5.0181184](https://doi.org/10.1063/5.0181184)

Submitted: 15 October 2023 · Accepted: 2 January 2024 ·

Published Online: 17 January 2024



View Online



Export Citation



CrossMark

Saikat Maji, Kartikey Pratap Chauhan, Ishan Bhat, Ankan Mukhopadhyay, Soubhik Kayal, and P. S. Anil Kumar

AFFILIATIONS

Department of Physics, Indian Institute of Science, Bangalore 560012, India

^{a)} Author to whom correspondence should be addressed: anil@iisc.ac.in

ABSTRACT

The spin current can be generated by passing an electric current through a heavy metal. The spin current generation depends on the spin Hall angle (θ_{sh}) of the material. To manipulate the effective θ_{sh} , a thin layer of Au has been introduced at the bottom Pt/Co and the top Co/Pt interfaces in Ta/Pt/Co/Pt based perpendicularly magnetic anisotropy systems, and current-induced magnetization reversal of Co has been studied to estimate J_c . The introduction of the Au layer at the top Co/Pt interface (Ta/Pt/Co/Au/Pt) did not produce any significant reduction in the J_c . However, a significant reduction of J_c ($\sim 34\%$) has been observed, while the Au layer has been deposited at the bottom Pt/Co interface (Ta/Pt/Au/Co/Pt), indicating an enhancement in the value of θ_{sh} . We also performed a micromagnetic simulation to understand the qualitative change of the θ_{sh} . Micromagnetic simulation suggested that the θ_{sh} becomes 0.07 in Ta/Pt/Au/Co/Pt multilayer compared to $\theta_{sh} = 0.05$ of the Ta/Pt/Co/Pt system. Pt/Co/Au/Co/Au exhibits a reduction in J_c up to $\sim 30\%$ and corresponds to $\theta_{sh} = 0.09$. A Ta capping layer has been introduced to inject more spin current into the Co layer since Pt and Ta have opposite spin Hall angles. The J_c lowers up to $\sim 58\%$ in Ta/Pt/Au/Co/Pt/Ta multilayer, corresponding to $\theta_{sh} = 0.23$. We also achieved field-free switching at $J_c = 1.55 \times 10^{11}$ by depositing an in-plane magnetized layer of Co in Ta/Pt/Au/Co/Pt/Ta/Co/Pt multilayer.

Published under an exclusive license by AIP Publishing. <https://doi.org/10.1063/5.0181184>

Heavy metal (HM)/ferromagnet (FM)/heavy metal and HM/FM/metal-oxide multilayer thin films are widely studied since they exhibit remarkable interfacial properties. The surface anisotropy dominates over the bulk anisotropy at the HM/FM interface to realize the perpendicularly magnetic anisotropy (PMA) system in which the easy axis of magnetization lies perpendicular to the film plane. The PMA systems are known to host chiral domain walls of Néel type^{1–6} and other complicated spin-textures^{7–11} supported by the interfacial Dzyaloshinskii–Moriya interaction (iDMI),^{12–15} which is also emerging from the HM/FM interface.^{16,17} The HM layer converts an applied longitudinal charge current (\mathbf{J}_q) to a transverse spin current (\mathbf{J}_s) of the fixed direction of spin polarization ($\hat{\sigma}$) due to the spin Hall effect (SHE). This charge-to-spin conversion ratio is characterized by the spin Hall angle (θ_{sh}) and expressed as $\theta_{sh} = (2e/\hbar) J_s/J_q$. The direction of spin polarization of the generated spin current is given by $\hat{\sigma} = \hat{\mathbf{J}}_q \times \hat{\mathbf{J}}_s$. Injection of this spin-polarized current into an adjacent FM layer applies spin-orbit torque (SOT) on the magnetization of the FM layer to

manipulate the magnetization. The SOT-driven domain walls and skyrmions can achieve very high velocity in the PMA systems.

The current-induced magnetization reversal (CIMR) in the PMA systems^{18–21} using SOT attained immense attraction for their potential use in nonvolatile memory devices. The spin-polarized current generally gives rise to two SOT terms in the magnetization dynamics governed by the Landau–Lifshitz–Gilbert (LLG) equation. Both of these two SOT terms are magnetization ($\hat{\mathbf{m}}$) dependent^{22,23} and often labeled as field-like torque ($\tau_{FL} \sim J_q \hat{\mathbf{m}} \times \hat{\sigma}$) and damp-like torque ($\tau_{DL} \sim J_q \hat{\mathbf{m}} \times \hat{\sigma} \times \hat{\mathbf{m}}$). The strength of the SOT also depends on the θ_{sh} of the HM layer. It is, therefore, desirable to have a large θ_{sh} to enhance the performance of the SOT-based devices. Different combinations of HM/FM^{18,24–28} and HM-alloy/FM^{29,30} interfaces have been investigated in the recent past to evaluate θ_{sh} . It has been observed that HMs like Ta, Pt, W, Pd, etc., have large θ_{sh} because of their significant spin-orbit coupling strength. The HM/FM interface plays a major role in SOT strength as there can be spin memory loss^{31,32} or the spin

backflow³³ at the interface, lowering the θ_{sh} of HM/FM interface. In HM/FM/FM based PMA systems, the top HM layer acts as a capping layer. The top and bottom HM layers can generate spin currents of opposite polarization, thus reducing the spin current available for producing SOT. To distinguish the independent contribution to the spin current arising from the top and bottom heavy metal layers, the term effective θ_{sh} has been introduced. The effective θ_{sh} can be treated as the spin Hall angle of the multilayer. Also, two different HMs with opposite signs of θ_{sh} have been introduced on both sides of the FM layer^{34–38} to enhance the system’s effective θ_{sh} . In this work, Ta/Pt/Co/X multilayers with different capping layers (X = Pt, Au, Ta) were investigated to estimate critical current density of magnetization switching. We deposited three samples, namely, M1 (Ta/Pt/Co/Pt), M2 (Ta/Pt/Co/Au/Pt), and M3 (Ta/Pt/Au/Co/Pt) for X = Pt. The Au layer has been introduced to modify the top Co/Pt and bottom Pt/Co interfaces in M2 and M3, respectively. For X = Au, two samples were prepared, one with Au as a capping layer denoted as M4 (Ta/Pt/Co/Au) and another with an Au layer introduced at the bottom Pt/Co interface denoted as M5 (Ta/Pt/Au/Co/Au). Three samples were prepared for X = Ta. The three samples are denoted as M6 (Ta/Pt/Co/Pt/Ta), M7 (Ta/Pt/Au/Co/Pt/Ta), and M8 (Ta/Pt/Au/Co/Pt/Ta/Co/Pt). The schematic diagram of all the samples has been presented in Fig. 1.

All samples presented in Fig. 1 were deposited on oxidized silicon wafer (with 280 nm SiO₂) using D.C. magnetron sputtering technique at room temperature at an Argon pressure of 5×10^{-3} mbar. A digital thickness monitor (DTM) monitored the growth rate of each layer kept very near to the substrate. The uniformity of the deposited films was ensured by rotating the substrate with a stepper motor at a rotation speed of 30 rpm. The average growth rate of Pt, Ta, Au, and Co was 0.044, 0.030, 0.069, and 0.019 nm/s, respectively. X-ray reflectivity (XRR) measurements were carried out to quantify the thickness and interface roughness of all samples (details in Fig. S1). Magnetic characterizations were performed using the vibrating sample magnetometry (VSM) technique at room temperature (Fig. S2). The CIMR measurements have been carried out after patterning the samples into 100 μm long and 10 μm wide devices prepared by standard photo-lithography technique followed by Ar-ion etching (Fig. S4). To perform CIMR measurements, the samples were first saturated by applying a large out-of-plane (OP) magnetic field (H_z), and variable current pulses of pulse width 50 μs were then applied from a Keithley 6221 current source in the presence of an in-plane (IP) magnetic field (H_x) to determine the switching current density (J_c). The current density is calculated by dividing the current by the cross-sectional area

							Pt
							Co →
							Ta
Pt	Au	Co ↑	Au	Au	Ta	Pt	Pt
Co ↑	Co ↑	Au	Co ↑	Co ↑	Co ↑	Co ↑	Co ↑
Pt	Pt	Pt	Pt	Pt	Pt	Pt	Pt
Ta	Ta	Ta	Ta	Ta	Ta	Ta	Ta
Si/SiO ₂	Si/SiO ₂	Si/SiO ₂	Si/SiO ₂	Si/SiO ₂	Si/SiO ₂	Si/SiO ₂	Si/SiO ₂
M1	M2	M3	M4	M5	M6	M7	M8

FIG. 1. Schematic diagram of the prepared samples. The magnetization of the Co layer has been indicated by the arrows.

(multilayer thickness \times device width) of the devices. The magnetization states were captured using the differential Kerr microscopy technique in the polar mode. We also performed micromagnetic simulations using Ubermag, an OOMMF-based python package.^{39,40}

The current-induced magnetization switching in PMA systems can be explained from the domain wall dynamics of chiral Néel walls under the influence of SOTs. The inversion asymmetry at the HM/FM interface generates iDMI that stabilizes the Néel wall with chirality fixed by the direction of the effective iDMI field (H_{DMI}). The effective fields associated with τ_{FL} and τ_{DL} can be represented as $\mathbf{H}_{\text{FL}} \sim -\hat{\sigma}$ and $\mathbf{H}_{\text{DL}} \sim -\hat{\sigma} \times \hat{\mathbf{m}}$, respectively. \mathbf{H}_{DL} , also named as the anti-damping field, is the most relevant term that takes part in magnetization switching. The magnetization reversal can be explained as a two-step process.^{41,42} The first step involves the current-induced nucleation of reversed domains of smaller size. In the second step, the SOT-driven motion of the Néel wall in the presence of H_x takes place, and the magnetization reverses. The details of the switching process are depicted in Fig. 2. In Fig. 2, a domain with magnetization, $-M_z$, is nucleated in a completely saturated FM layer of magnetization, $+M_z$. The Néel type of domain wall is formed, and the chirality is fixed according to the sign of H_{DMI} . When current is applied, the H_{DL} acting on the moment inside the domain wall is represented as H_z^{eff} , and the direction of IP field ($H_x = 0$), both the domain walls have same velocity (v_{DW}) in the same direction [Fig. 2(a)]. The domain wall motion is observed in this case. Thus, magnetization reversal is not realized for $H_x = 0$. When the H_x is applied along the $+x$ direction, the moments inside the domain wall align with the IP field, and the H_z^{eff} on both the moments is directed along the $-z$ direction. Both the domain walls will have velocities in the direction shown in Fig. 2(b). Here, the velocities of the domain walls lead to the expansion of the nucleated domain. As a result, the magnetization reverses to $-M_z$ from $+M_z$. The magnetization reversal can be seen in this case. On the contrary, as the current direction is reversed, the H_z^{eff} on the moments inside both walls also reverses toward $+H_z$. The nucleated domain will shrink according to the direction of v_{DW} , and final magnetization attains the $+M_z$ state [Fig. 2(c)]. This explains that the IP bias field (H_x) parallel to the current direction is necessary for magnetization reversal. Also, the magnetization reversal from $+M_z$ to $-M_z$ can be seen only for $+H_x$ and $+J_x$. Similarly, if the FM layer is initially saturated along $-M_z$, the reversal to the $+M_z$ state requires $+H_x$ and $-J_x$. The magnetization state with respect to current density (J) has been shown in Fig. 3(a).

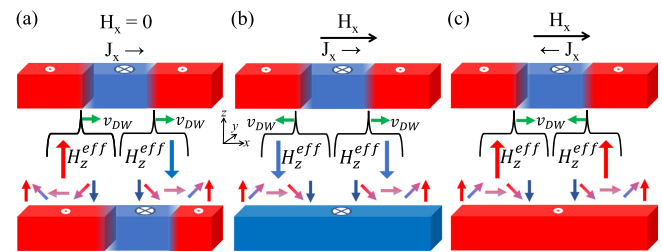


FIG. 2. The magnetization reversal process. (a) The current-induced domain wall motion for $H_x = 0$. The domain expansion in the presence of (b) H_x and $J_x > 0$ and (c) H_x and $J_x < 0$. The magnetization configuration inside the domain wall has been shown to find out the H_{DL} acting on moment inside the domain wall (H_z^{eff}). The direction of H_z^{eff} has been indicated with the arrows. Also, the domain wall velocities (v_{DW}) have been marked to understand the reversal process.

The J_c of the samples (M1, M2, and M3), (M4 and M5), (M6 and M7), and M8 as a function of H_x has been displayed in Figs. 3(b), 3(c), 3(d), and 3(f), respectively. The J_c lowers with an increase in H_x for all the samples. The maximum $J_c (= 3.13 \times 10^{11} \text{ A/m}^2)$ has been observed for the sample M1 at $H_x = 100 \text{ mT}$. At the same H_x , the $J_c (= 2.96 \times 10^{11} \text{ A/m}^2)$ becomes slightly lesser for the sample M2. In Pt/Co/Pt systems, spin-polarized currents of the same polarity are introduced to the Co layer from the bottom and top Pt layers. As a result, the effective θ_{sh} of the system reduces and results in a high J_c value for the magnetization reversal. In M1, the spin-polarized electrons with opposite $\hat{\sigma}$ have been injected into the Co layer from bottom Pt/Co and top Co/Pt interfaces, and the higher J_c is observed for M1. However, the behavior differs at $H_x = 10 \text{ mT}$. At $H_x = 10 \text{ mT}$, the $J_c (= 3.69 \times 10^{11} \text{ A/m}^2)$ for the sample M2 is slightly higher than the $J_c (= 3.56 \times 10^{11} \text{ A/m}^2)$ of the sample M1. This behavior at a lower IP magnetic field cannot be explained with the help of effective θ_{sh} alone. In addition, M2 has higher D_{eff} than M1⁶ that can also play a significant role in explaining the reduction of the J_c as well as the nature of J_c vs H_x graph. For the sample M3, the J_c reduces to $2.35 \times 10^{11} \text{ A/m}^2$ at $H_x = 10 \text{ mT}$, which is $\sim 34\%$ reduction in J_c with respect to the sample M1. In sample M4, magnetization reversal has been observed for $J_c = 3.46 \times 10^{11} \text{ A/m}^2$ at $H_x = 10 \text{ mT}$. The sample M6 comprises Pt/Co and Co/Au interfaces, where only the Pt layer generated electrons through the spin Hall effect instead of the Au layer that contributes negligibly small spin current.⁴⁵ The effective θ_{sh}

is expected to be large in M4.⁴³ However, we only observed $\sim 8\%$ reduction of J_c as compared to the sample M1 at $H_x = 10 \text{ mT}$, which suggests the effective θ_{sh} is not large enough compared to the sample M1. This might be because of the fact that the top Pt layer is very thin (thickness $\sim 1 \text{ nm}$) in M1 and does not generate many spin-polarized electrons. The asymmetric cancellation of spin current from bottom Pt/Co and top Co/Pt gives rise to sufficient SOT to switch the magnetization of sample M1 at $J_c = 3.56 \times 10^{11} \text{ A/m}^2$. It has been confirmed in an earlier report that even the symmetric thickness of Pt in the Pt/Co/Pt system deposited on the SiO_2 substrate can have non-zero field-like and damp-like torque⁴⁶ to realize magnetization switching. Thus, capping with the Au layer does not reduce the J_c much in the sample M4. The current density was reduced to $J_c = 2.49 \times 10^{11} \text{ A/m}^2$ at $H_x = 10 \text{ mT}$ in the sample M5, which is $\sim 30\%$ reduction in J_c compared to the sample M4. The modification of the bottom Pt/Co interface with the introduction of the Au layer in both the Ta/Pt/Co/Pt and Ta/Pt/Co/Au multilayers enhances the effective θ_{sh} and results in a significant reduction of J_c compared to the modification of top Co/Pt interface with the Au layer. The samples M3 and M5 have similar layer configurations except the capping layer. The M5 is expected to have lower J_c as the capping layer is Au as opposed to M3, where cancellation of spin current is possible by the spin current generated from the Pt capping layer. However, we observed a higher J_c for the sample M5. Sample M3 has more asymmetry around the Co layer than the sample M5. So, the DMI of sample M5 is expected to be lower than that of the

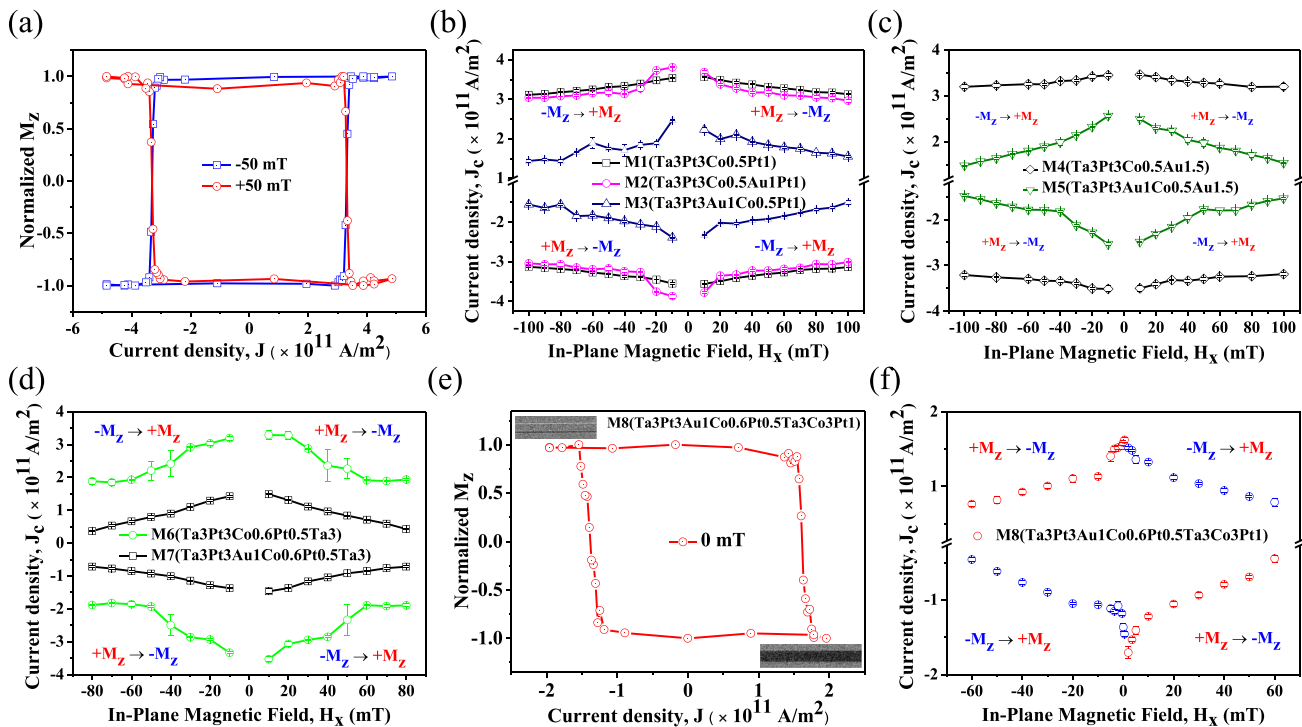


FIG. 3. (a) The magnetization reversal as a function of current density at $H_x = -50$ and $H_x = +50 \text{ mT}$ of the sample M1. The current (J_c) required for magnetization reversal as a function of in-plane bias magnetic field (H_x) of (b) M1, M2, and M3, (c) M4 and M5, and (d) M6 and M7. The switching from $+M_z$ state to $-M_z$ has been observed for $(-J_x, +H_x)$ for all the samples. (e) The field-free magnetization reversal as a function of current density at $H_x = 0 \text{ mT}$ of the sample M8. The images taken from a differential Kerr microscope of the fabricated device have been shown in the inset. The darker (brighter) pixels represent the magnetization corresponding to $-M_z$ ($+M_z$) state. (f) J_c with respect to H_x of M8. The switching from $-M_z$ state to $+M_z$ has been observed for $(+J_x, +H_x)$ as opposed to other samples.

sample M3. The lower value of D_{eff} may result in a high J_c in M5. To further investigate the effect of the Au layer introduced at the bottom Pt/Co interface and reduce the current density of magnetization reversal, we have introduced the Ta capping layer that is known to have a negative spin Hall angle in the sample M7. To compare the reduction of the J_c of M7, we also deposited M6. A thin Pt layer of thickness 0.5 nm has been introduced between the top Co and Ta layers to improve the interface quality and achieve PMA. The Pt layer thickness has been kept lower to minimize the spin current generation from this layer. The introduction of spin current with same spin polarization ($\hat{\sigma}$) from both sides of the Co layer reduces the J_c to 3.29×10^{11} A/m² in the sample M6 [Fig. 3(d)]. The introduction of the Au layer at the bottom Pt/Co interface leads to $\sim 55\%$ reduction of J_c ($= 1.48 \times 10^{11}$ A/m²) in the sample M7 with respect to M6. The reduction of J_c can be attributed to the improvement of spin transparency of Pt/Au/Co interface leading to an increase in effective θ_{sh} of the system. In the Pt/Co interface, the spin current faces more dephasing⁴⁷ due to proximity-induced magnetization (PIM) in the Pt.^{48,49} Introduction of the Au layer reduces the PIM in the Pt,⁵⁰ which leads to less dephasing of spin current,⁵¹ and the spin transparency of Pt/Au/Co interface increases with respect to the Pt/Co interface.⁴⁷ To achieve field-free switching, we prepared sample M8 with an additional in-plane magnetized (IMA) Co layer of 3 nm on top of the Ta layer. The magnetization states captured by the Kerr microscope reveal the deterministic switching of magnetization at $H_x = 0$ mT as shown in Fig. 3(e). The sample was pre-magnetized with $H_x = -30$ mT, and then H_x was removed before the current-induced measurement. The current density for field-free switching has been observed at $J_c = 1.55 \times 10^{11}$ A/m². The IMA and PMA layers of Co are coupled through interlayer exchange coupling (IEC). The IEC introduces an in-plane magnetic field H_{IEC} in the direction opposite to the magnetization of the IMA layer. The IEC has been observed in Ta/Pt/Co/Ta/Co/Pt multilayer.⁵² The H_{IEC} tilts the magnetization of the PMA layer, and field-free switching was observed. The switching sense observed here was different from the other samples [Fig. 3(a)] due to the H_{IEC} (details in Fig. S5). The variation of J_c with H_x has been presented in Fig. 3(f). At $H_x = 10$ mT, the J_c ($= 1.33 \times 10^{11}$) reduced up to $\sim 60\%$ with respect to M4.

To understand the role of iDMI and spin Hall angle in magnetization reversal, micromagnetic simulation has been performed, solving

the Landau–Lifshitz–Gilbert–Slonczewski equation with the damping constant, $\alpha = 0.5$,⁵³ and the exchange stiffness constant, $A = 1.6 \times 10^{-11}$.^{1,5} The magnetic properties (M_s , K_{eff}) of the samples as obtained from the experiment have been defined in the simulations. The iDMI strength (D_{eff}) and the spin Hall angle (θ_{sh}) have been varied to compare the experimental results. The simulation results suggested that the increase in D_{eff} or θ_{sh} leads to a reduction in J_c (Fig. S6). The J_c as a function of H_x obtained from simulations has been displayed in Fig. 4. All the simulation parameters have been summarized in Table I. For the simulation of J_c of the sample M1, the parameters have been chosen as $D_{\text{eff}} = 0.25$ mJ/m² (Ref. 6) and $\theta_{sh} = 0.05$ (Refs. 54 and 55) from the literature. It has been previously observed that the D_{eff} increases with the introduction of the Au layer at the top Co/Pt interface in M2. To simulate J_c of M2, the D_{eff} (~ 0.75 mJ/m²) has been taken from the literature for similar sample.⁶ The $\theta_{sh} = 0.042$ was obtained from the simulations to match the % reduction of J_c with the experimental results. To understand the reduction in J_c for M3, the simulations were first carried out by fixing $\theta_{sh} = 0.05$ and varying the D_{eff} . $D_{\text{eff}} \sim 2.00$ mJ/m² was obtained from simulation to match up for the 30% reduction in J_c (Fig. S6). The D_{eff} in these multilayers can be visualized from the three-atom model proposed by Yang *et al.*,¹⁷ where the DMI is introduced in FM atom from nearby HM atoms. As shown in the literature, the D_{eff} of the Au/Co interface is much smaller than Pt/Co interface.^{17,56,57} In the case of M3, since an Au layer is introduced at the bottom Pt/Co interface, it is very difficult to justify such a high magnitude of D_{eff} for Ta/Pt/Au/Co/Pt multilayer obtained from simulation. Thus, to simulate J_c vs H_x , we have fixed an intermediate value of $D_{\text{eff}} = 0.50$ mJ/m² and obtained $\theta_{sh} = 0.07$ to achieve $\sim 36\%$ reduction in J_c (Fig. S6). The $D_{\text{eff}} = 1.00$ mJ/m² (Ref. 43) has been chosen for the simulation of M4, and the $\theta_{sh} = 0.064$ was obtained from simulations. The simulation suggests an increment in θ_{sh} of M4 compared to M1, consistent with our discussion of spin current generation described earlier. In M5, we have taken a moderate value of D_{eff} since both sides of the Co layer consist of the Au layer. The $\theta_{sh} = 0.09$ was obtained from the simulations. Similarly for M6, the $D_{\text{eff}} = 1.10$ mJ/m² has been taken from the literature.^{38,44,58} The $\theta_{sh} = 0.09$ was obtained for the sample M6, and this value agrees well with the literature.³⁸ One important point to note here is that though the J_c of M6 has been reduced only 7% with respect to M1, the θ_{sh} of M6 increased significantly. This can be attributed to the fact that the

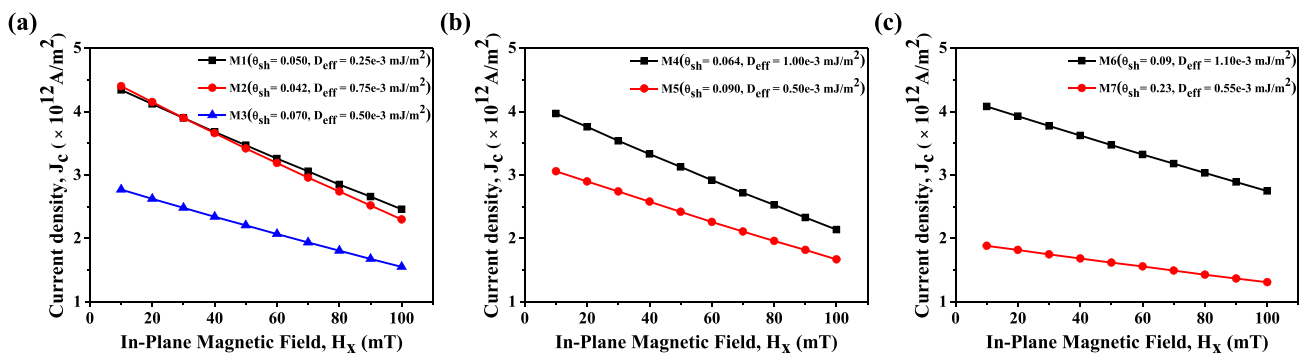


FIG. 4. Simulation results of switching current density (J_c) as a function of in-plane magnetic (H_x) of (a) M1 (Ta/Pt/Co/Pt), M2 (Ta/Pt/Co/Au/Pt) and M3 (Ta/Pt/Au/Co/Pt), (b) M4 (Ta/Pt/Co/Au) and M5 (Ta/Pt/Au/Co/Au), and (c) M6 (Ta/Pt/Co/Pt/Ta) and M7 (Ta/Pt/Au/Co/Pt/Ta).

TABLE I. The simulation parameters. The reduction of J_c has been calculated with respect to the J_c of sample M1 at $H_x = 10$ mT. The θ_{sh} values have been extracted to match the percentage of reduction of J_c with the experiment (Expt.).

Sample	Multilayered heterostructures deposited on Si/SiO ₂	iDMI strength, D_{eff} (mJ/m ²)	$J_c \times 10^{12}$ (A/m ²)	Reduction in J_c		θ_{sh} from simulation
				Expt.	Simulation	
M1	Ta/Pt/Co/Pt	0.25 (Ref. 6)	4.34	0.05
M2	Ta/Pt/Co/Au/Pt	0.75 (Ref. 6)	4.40	0.042
M3	Ta/Pt/Au/Co/Pt	0.50	2.77	34	36	0.07
M4	Ta/Pt/Co/Au	1.00 (Ref. 43)	3.97	8	8	0.064
M5	Ta/Pt/Au/Co/Au	0.50	3.06	30	30	0.09
M6	Ta/Pt/Co/Pt/Ta	1.10 (Ref. 44)	4.08	7	7	0.09
M7	Ta/Pt/Au/Co/Pt/Ta	0.55	2.16	58	57	0.23
M8	Ta/Pt/Au/Co/Pt/Ta/Co/Pt	NA	NA	62	NA	NA

K_{eff} of M6 is higher than M1 (Table S2). Again for the sample M7, a moderate value of $D_{\text{eff}} = 0.55$ mJ/m² has been considered for simulation, and $\theta_{sh} = 0.23$ was obtained to match up with the $\sim 57\%$ reduction of J_c . The extracted values of θ_{sh} cannot be treated as the absolute value of the multilayers since the effect of disorder and Joule heating has not been included in the simulation (more detail in Sec. S6).

In conclusion, three sets of PMA samples were prepared to study the current-induced magnetization switching. One set involves Ta/Pt/Co/Pt based multilayers where the top Co/Pt and bottom Pt/Co interface have been modified by depositing an Au spacer layer to prepare Ta/Pt/Co/Au/Pt and Ta/Pt/Au/Co/Pt, respectively. Another set comprises Ta/Pt/Co/Au and Ta/Pt/Au/Co/Au multilayers. The third set consists of three samples, Ta/Pt/Co/Pt/Ta, Ta/Pt/Au/Co/Pt/Ta, and Ta/Pt/Au/Co/Pt/Ta/Co/Pt. The CIMR study suggested that the current density of magnetization switching (J_c) can be lowered significantly when the Au layer is introduced at the bottom Pt/Co interface. The reduction of J_c up to $\sim 58\%$ has been observed for Ta/Pt/Au/Co/Pt/Ta sample as compared to the Ta/Pt/Co/Pt sample. The field-free magnetization switching was also observed in Ta/Pt/Au/Co/Pt/Ta/Co/Pt multilayers for $J_c = 1.55 \times 10^{11}$ A/m². We also performed micromagnetic simulations to estimate the effective spin Hall angle of the multilayers, defining simulation parameters from literature and experiments. Our study demonstrates an alternative way to manipulate the effective spin Hall angle of PMA systems to reduce the J_c , which will be immensely helpful for constructing high-density magnetic data storage devices.

See the supplementary material for the details of XRR fitting, magnetic measurement, the device, the effect of Joule heating, field-free switching, and micromagnetic simulation.

We would like to thank Mr. Tarun Maity for his immense help in conducting micromagnetic simulations. We also thank Professor Kyung-Jin Lee for the fruitful discussion on micromagnetic simulations. We acknowledge the National Nano-fabrication Center, Centre for Nano Science and Engineering (CeNSE) for the clean-room facility and the Micro-Nano Characterization Facility, CeNSE, for measurement facilities. S.M. and A.M. would like to thank the Ministry of Education (MoE), India, and S.K. would like to thank the Council of Scientific and Industrial Research (CSIR)

for the research fellowship. P.S.A.K. gratefully acknowledges DST-SERB for the financial support.

AUTHOR DECLARATIONS

Conflict of Interest

The authors have no conflicts to disclose.

Author Contributions

Saikat Maji: Conceptualization (equal); Data curation (lead); Formal analysis (lead); Investigation (lead); Methodology (equal); Validation (lead); Writing – original draft (lead). **Kartikey Pratap Chauhan:** Data curation (equal); Formal analysis (equal); Investigation (equal); Validation (equal); Writing – review & editing (equal). **Ishan Bhat:** Data curation (equal); Investigation (equal); Validation (equal); Writing – review & editing (equal). **Ankan Mukhopadhyay:** Conceptualization (equal); Data curation (equal); Formal analysis (equal); Investigation (equal); Validation (equal); Writing – review & editing (equal). **Soubhik Kayal:** Conceptualization (equal); Data curation (equal); Formal analysis (equal); Investigation (equal); Validation (equal); Writing – review & editing (equal). **P. S. Anil Kumar:** Conceptualization (equal); Funding acquisition (lead); Project administration (lead); Resources (lead); Supervision (lead); Writing – review & editing (equal).

DATA AVAILABILITY

The data that support the findings of this study are available from the corresponding author upon reasonable request.

REFERENCES

- ¹A. Thiaville, S. Rohart, É. Jué, V. Cros, and A. Fert, "Dynamics of Dzyaloshinskii domain walls in ultrathin magnetic films," *Europhys. Lett.* **100**, 57002 (2012).
- ²K.-W. Kim, H.-W. Lee, K.-J. Lee, and M. D. Stiles, "Chirality from interfacial spin-orbit coupling effects in magnetic bilayers," *Phys. Rev. Lett.* **111**, 216601 (2013).
- ³S. Emori, U. Bauer, S.-M. Ahn, E. Martinez, and G. S. Beach, "Current-driven dynamics of chiral ferromagnetic domain walls," *Nat. Mater.* **12**, 611 (2013).
- ⁴K.-S. Ryu, L. Thomas, S.-H. Yang, and S. Parkin, "Chiral spin torque at magnetic domain walls," *Nat. Nanotechnol.* **8**, 527 (2013).

- ⁵A. Hrabec, N. A. Porter, A. Wells, M. J. Benitez, G. Burnell, S. McVitie, D. McGrouther, T. A. Moore, and C. H. Marrows, "Measuring and tailoring the Dzyaloshinskii-Moriya interaction in perpendicularly magnetized thin films," *Phys. Rev. B* **90**, 020402 (2014).
- ⁶S. Maji, A. Mukhopadhyay, S. Kayal, and P. S. Anil Kumar, "Domain wall chirality reversal by interfacial engineering in Pt/Co/Pt based perpendicularly magnetized systems," *J. Appl. Phys.* **133**, 023907 (2023).
- ⁷Y. Ishikawa, K. Tajima, D. Bloch, and M. Roth, "Helical spin structure in manganese silicide MnSi," *Solid State Commun.* **19**, 525 (1976).
- ⁸A. Fert and P. M. Levy, "Role of anisotropic exchange interactions in determining the properties of spin-glasses," *Phys. Rev. Lett.* **44**, 1538 (1980).
- ⁹M. Bode, A. Sala, L. D. Buda-Prejbeanu, O. Klein *et al.*, "Room-temperature chiral magnetic skyrmions in ultrathin magnetic nanostructures," *Nat. Nanotechnol.* **11**, 449 (2016).
- ¹⁰W. Jiang, P. Upadhyaya, W. Zhang, G. Yu, M. B. Jungfleisch, F. Y. Fradin, J. E. Pearson, Y. Tserkovnyak, K. L. Wang, O. Heinonen *et al.*, "Blowing magnetic skyrmion bubbles," *Science* **349**, 283 (2015).
- ¹¹O. Boulle, J. Vogel, H. Yang, S. Pizzini, D. de Souza Chaves, A. Locatelli, T. O. Menteş, A. Sala, L. D. Buda-Prejbeanu, O. Klein *et al.*, "Room-temperature chiral magnetic skyrmions in ultrathin magnetic nanostructures," *Nat. Nanotechnol.* **11**, 449 (2016).
- ¹²I. Dzyaloshinsky, "A thermodynamic theory of 'weak' ferromagnetism of antiferromagnetics," *J. Phys. Chem. Solids* **4**, 241 (1958).
- ¹³T. Moriya, "Anisotropic superexchange interaction and weak ferromagnetism," *Phys. Rev.* **120**, 91 (1960).
- ¹⁴T. Moriya, "New mechanism of anisotropic superexchange interaction," *Phys. Rev. Lett.* **4**, 228 (1960).
- ¹⁵A. Crépeux and C. Lacroix, "Dzyaloshinsky-Moriya interactions induced by symmetry breaking at a surface," *J. Magn. Magn. Mater.* **182**, 341 (1998).
- ¹⁶A. Fert, V. Cros, and J. Sampaio, "Skyrmions on the track," *Nat. Nanotechnol.* **8**, 152 (2013).
- ¹⁷H. Yang, A. Thiaville, S. Rohart, A. Fert, and M. Chshiev, "Anatomy of Dzyaloshinskii-Moriya interaction at Co/Pt interfaces," *Phys. Rev. Lett.* **115**, 267210 (2015).
- ¹⁸L. Liu, O. J. Lee, T. J. Gudmundsen, D. C. Ralph, and R. A. Buhrman, "Current-induced switching of perpendicularly magnetized magnetic layers using spin torque from the spin Hall effect," *Phys. Rev. Lett.* **109**, 096602 (2012).
- ¹⁹I. M. Miron, K. Garello, G. Gaudin, P.-J. Zermatten, M. V. Costache, S. Auffret, S. Bandiera, B. Rodmacq, A. Schuhl, and P. Gambardella, "Perpendicular switching of a single ferromagnetic layer induced by in-plane current injection," *Nature* **476**, 189 (2011).
- ²⁰M. Jamali, K. Narayanapillai, X. Qiu, L. M. Loong, A. Manchon, and H. Yang, "Spin-orbit torques in Co/Pd multilayer nanowires," *Phys. Rev. Lett.* **111**, 246602 (2013).
- ²¹V. Mohanan, K. Ganesh, and P. A. Kumar, "Spin Hall effect mediated current-induced deterministic switching in all-metallic perpendicularly magnetized Pt/Co/Pt trilayers," *Phys. Rev. B* **96**, 104412 (2017).
- ²²J. Kim, J. Sinha, M. Hayashi, M. Yamanouchi, S. Fukami, T. Suzuki, S. Mitani, and H. Ohno, "Layer thickness dependence of the current-induced effective field vector in Ta[CoFeB]/MgO," *Nat. Mater.* **12**, 240 (2013).
- ²³K. Garello, I. M. Miron, C. O. Avci, F. Freimuth, Y. Mokrousov, S. Blügel, S. Auffret, O. Boulle, G. Gaudin, and P. Gambardella, "Symmetry and magnitude of spin-orbit torques in ferromagnetic heterostructures," *Nat. Nanotechnol.* **8**, 587 (2013).
- ²⁴C.-F. Pai, L. Liu, Y. Li, H. Tseng, D. Ralph, and R. Buhrman, "Spin transfer torque devices utilizing the giant spin Hall effect of tungsten," *Appl. Phys. Lett.* **101**, 122404 (2012).
- ²⁵L. Liu, C.-F. Pai, Y. Li, H. Tseng, D. Ralph, and R. Buhrman, "Spin-torque switching with the giant spin Hall effect of tantalum," *Science* **336**, 555 (2012).
- ²⁶C. Onur Avci, K. Garello, I. Mihai Miron, G. Gaudin, S. Auffret, O. Boulle, and P. Gambardella, "Magnetization switching of an MgO/Co/Pt layer by in-plane current injection," *Appl. Phys. Lett.* **100**, 212404 (2012).
- ²⁷C. Du, H. Wang, F. Yang, and P. C. Hammel, "Systematic variation of spin-orbit coupling with *d*-orbital filling: Large inverse spin Hall effect in 3*d* transition metals," *Phys. Rev. B* **90**, 140407 (2014).
- ²⁸Q. Hao and G. Xiao, "Giant spin Hall effect and switching induced by spin-transfer torque in a W/Co₄₀Fe₄₀B₂₀/MgO structure with perpendicular magnetic anisotropy," *Phys. Rev. Appl.* **3**, 034009 (2015).
- ²⁹Y. Niimi, Y. Kawanishi, D. H. Wei, C. Deranlot, H. X. Yang, M. Chshiev, T. Valet, A. Fert, and Y. Otani, "Giant spin Hall effect induced by skew scattering from bismuth impurities inside thin film CuBi alloys," *Phys. Rev. Lett.* **109**, 156602 (2012).
- ³⁰M. Obstbaum, M. Decker, A. K. Greitner, M. Haertinger, T. N. G. Meier, M. Kronseder, K. Chadova, S. Wimmer, D. Ködderitzsch, H. Ebert, and C. H. Back, "Tuning spin Hall angles by alloying," *Phys. Rev. Lett.* **117**, 167204 (2016).
- ³¹Y. Liu, Z. Yuan, R. J. H. Wesselink, A. A. Starikov, and P. J. Kelly, "Interface enhancement of Gilbert damping from first principles," *Phys. Rev. Lett.* **113**, 207202 (2014).
- ³²J.-C. Rojas-Sánchez, N. Reyren, P. Laczkowski, W. Savero, J.-P. Attané, C. Deranlot, M. Jamet, J.-M. George, L. Vila, and H. Jaffrès, "Spin pumping and inverse spin Hall effect in platinum: The essential role of spin-memory loss at metallic interfaces," *Phys. Rev. Lett.* **112**, 106602 (2014).
- ³³P. M. Haney, H.-W. Lee, K.-J. Lee, A. Manchon, and M. D. Stiles, "Current induced torques and interfacial spin-orbit coupling: Semiclassical modeling," *Phys. Rev. B* **87**, 174411 (2013).
- ³⁴S. Woo, M. Mann, A. J. Tan, L. Caretta, and G. S. Beach, "Enhanced spin-orbit torques in Pt/Co/Ta heterostructures," *Appl. Phys. Lett.* **105**, 212404 (2014).
- ³⁵K. Ueda, C.-F. Pai, A. J. Tan, M. Mann, and G. S. Beach, "Effect of rare earth metal on the spin-orbit torque in magnetic heterostructures," *Appl. Phys. Lett.* **108**, 232405 (2016).
- ³⁶J. Yu, X. Qiu, W. Legrand, and H. Yang, "Large spin-orbit torques in Pt/Co-Ni/W heterostructures," *Appl. Phys. Lett.* **109**, 042403 (2016).
- ³⁷J. Yun, D. Li, B. Cui, X. Guo, K. Wu, X. Zhang, Y. Wang, Y. Zuo, and L. Xi, "Spin-orbit torque induced magnetization switching in Pt/Co/Ta structures with perpendicular magnetic anisotropy," *J. Phys. D* **50**, 395001 (2017).
- ³⁸S. Kayal, S. Maji, A. Mukhopadhyay, and P. S. A. Kumar, "Enhancing the spin-orbit torque efficiency in Pt/CoFeB/Pt based perpendicularly magnetized system," *J. Magn. Magn. Mater.* **558**, 169499 (2022).
- ³⁹M. Beg, M. Lang, and H. Fangohr, "Ubermag: Toward more effective micro-magnetic workflows," *IEEE Trans. Magn.* **58**, 7300205 (2022).
- ⁴⁰M. Beg, R. A. Pepper, and H. Fangohr, "User interfaces for computational science: A domain specific language for OOMMF embedded in python," *AIP Adv.* **7**, 056025 (2017).
- ⁴¹O. J. Lee, L. Q. Liu, C. F. Pai, Y. Li, H. W. Tseng, P. G. Gowtham, J. P. Park, D. C. Ralph, and R. A. Buhrman, "Central role of domain wall depinning for perpendicular magnetization switching driven by spin torque from the spin Hall effect," *Phys. Rev. B* **89**, 024418 (2014).
- ⁴²C.-F. Pai, M. Mann, A. J. Tan, and G. S. D. Beach, "Determination of spin torque efficiencies in heterostructures with perpendicular magnetic anisotropy," *Phys. Rev. B* **93**, 144409 (2016).
- ⁴³A. Hrabec, K. Shahbazi, T. A. Moore, E. Martinez, and C. H. Marrows, "Tuning spin-orbit torques at magnetic domain walls in epitaxial Pt/Co/Pt_{1-x}Au_x trilayers," *Nanotechnology* **30**, 234003 (2019).
- ⁴⁴K. Shahbazi, J.-V. Kim, H. T. Nembach, J. M. Shaw, A. Bischof, M. D. Rossell, V. Jeudy, T. A. Moore, and C. H. Marrows, "Domain-wall motion and interfacial Dzyaloshinskii-Moriya interactions in Pt/Co/Ir(t_r)/Ta multilayers," *Phys. Rev. B* **99**, 094409 (2019).
- ⁴⁵K.-S. Ryu, S.-H. Yang, L. Thomas, and S. S. P. Parkin, "Chiral spin torque arising from proximity-induced magnetization," *Nat. Commun.* **5**, 3910 (2014).
- ⁴⁶H. An, H. Nakayama, Y. Kanno, A. Nomura, S. Haku, and K. Ando, "Spin-orbit torques in asymmetric Pt/Co/Pt structures," *Phys. Rev. B* **94**, 214417 (2016).
- ⁴⁷C. Swindells, H. Głowiński, Y. Choi, D. Haskel, P. Michałowski, T. Hase, P. Kuświk, and D. Atkinson, "Proximity-induced magnetism and the enhancement of damping in ferromagnetic/heavy metal systems," *Appl. Phys. Lett.* **119**, 152401 (2021).
- ⁴⁸W. L. Lim, N. Ebrahim-Zadeh, J. Owens, H. G. Hentschel, and S. Urazhdin, "Temperature-dependent proximity magnetism in Pt," *Appl. Phys. Lett.* **102**, 162404 (2013).
- ⁴⁹A. Mukhopadhyay, S. K. Vayalil, D. Graulich, I. Ahamed, S. Francoual, A. Kashyap, T. Kuschel, and P. A. Kumar, "Asymmetric modification of the magnetic proximity effect in Pt/Co/Pt trilayers by the insertion of a Ta buffer layer," *Phys. Rev. B* **102**, 144435 (2020).

- ⁵⁰E. Montoya, T. McKinnon, A. Zamani, E. Girt, and B. Heinrich, "Broadband ferromagnetic resonance system and methods for ultrathin magnetic films," *J. Magn. Magn. Mater.* **356**, 12 (2014).
- ⁵¹P. Omelchenko, E. Girt, and B. Heinrich, "Test of spin pumping into proximity-polarized Pt by in-phase and out-of-phase pumping in Py/Pt/Py," *Phys. Rev. B* **100**, 144418 (2019).
- ⁵²Y. Sheng, K. W. Edmonds, X. Ma, H. Zheng, and K. Wang, "Adjustable current-induced magnetization switching utilizing interlayer exchange coupling," *Adv. Electron. Mater.* **4**, 1800224 (2018).
- ⁵³P. J. Metaxas, J. P. Jamet, A. Mougin, M. Cormier, J. Ferré, V. Baltz, B. Rodmacq, B. Dieny, and R. L. Stamps, "Creep and flow regimes of magnetic domain-wall motion in ultrathin Pt/Co/Pt films with perpendicular anisotropy," *Phys. Rev. Lett.* **99**, 217208 (2007).
- ⁵⁴C.-F. Pai, Y. Ou, L. H. Vilela-Leão, D. C. Ralph, and R. A. Buhrman, "Dependence of the efficiency of spin Hall torque on the transparency of Pt/ferromagnetic layer interfaces," *Phys. Rev. B* **92**, 064426 (2015).
- ⁵⁵X. Tao, Q. Liu, B. Miao, R. Yu, Z. Feng, L. Sun, B. You, J. Du, K. Chen, S. Zhang, L. Zhang, Z. Yuan, D. Wu, and H. Ding, "Self-consistent determination of spin Hall angle and spin diffusion length in Pt and Pd: The role of the interface spin loss," *Sci. Adv.* **4**, eaat1670 (2018).
- ⁵⁶V. Kashid, T. Schena, B. Zimmermann, Y. Mokrousov, S. Blügel, V. Shah, and H. G. Salunke, "Dzyaloshinskii-Moriya interaction and chiral magnetism in $3d-5d$ zigzag chains: Tight-binding model and *ab initio* calculations," *Phys. Rev. B* **90**, 054412 (2014).
- ⁵⁷H. Yang, O. Boule, V. Cros, A. Fert, and M. Chshiev, "Controlling Dzyaloshinskii-Moriya interaction via chirality dependent atomic-layer stacking, insulator capping and electric field," *Sci. Rep.* **8**(1), 12356 (2018).
- ⁵⁸S. Woo, K. Litzius, B. Krüger, M.-Y. Im, L. Caretta, K. Richter, M. Mann, A. Krone, R. M. Reeve, M. Weigand *et al.*, "Observation of room-temperature magnetic skyrmions and their current-driven dynamics in ultrathin metallic ferromagnets," *Nat. Mater.* **15**, 501 (2016).